

# Beyond Two Dark Energy Parameters

Devdeep Sarkar<sup>1</sup>, Scott Sullivan<sup>1</sup>, Shahab Joudaki<sup>1</sup>, Alexandre Amblard<sup>1</sup>, Daniel E. Holz<sup>2,3</sup>, and Asantha Cooray<sup>1</sup>

<sup>1</sup>*Department of Physics and Astronomy, University of California, Irvine, CA 92697*

<sup>2</sup>*Theoretical Division, Los Alamos National Laboratory, Los Alamos, NM 87545 and*

<sup>3</sup>*Department of Astronomy & Astrophysics, University of Chicago, Chicago, IL 60637*

(Dated: October 29, 2018)

Our ignorance of the dark energy is generally described by a two-parameter equation of state. In these approaches a particular *ad hoc* functional form is assumed, and only two independent parameters are incorporated. We propose a model-independent, multi-parameter approach to fitting the dark energy, and show that next-generation surveys will constrain the equation of state in three or more independent redshift bins to better than 10%. Future knowledge of the dark energy will surpass two numbers (e.g.,  $[w_0, w_1]$  or  $[w_0, w_a]$ ), and we propose a more flexible approach to the analysis of present and future data.

Standard candles such as Type Ia supernovae (SNe), as well as standard rulers such as the cosmic microwave background (CMB) and the baryon acoustic oscillation (BAO) scale, are currently the preferred probes of the expansion history of the Universe [1, 2, 3, 4]. By determining distances at cosmological scales, these probes have firmly established that the expansion of the universe is accelerating [5, 6, 7, 8]. It is now believed that a mysterious dark energy component with an energy density  $\sim 70\%$  of the total energy density of the universe is responsible for this accelerated expansion. The underlying physics of dark energy remains obscure [9] and understanding the acceleration has become one of the foremost challenges in fundamental physics.

In an attempt to discriminate observationally between differing models of dark energy, it is useful to parameterize the dark energy by its equation of state (EOS), encapsulating the ratio of pressure to density. When model fitting data, it is generally assumed that the dark energy EOS follows a certain predetermined evolutionary history with redshift,  $w(z)$ . Common parameterizations include a linear variation,  $w(z) = w_0 + w_z z$  [10], or an evolution that asymptotes to a constant  $w$  at high redshift,  $w(a) = w_0 + w_a(1 - a)$ , with  $a$  the scale factor [11, 12].

Fitting data to an assumed functional form leads to possible biases in the determination of properties of the dark energy and its evolution, especially if the true behavior of the dark energy EOS differs significantly from the assumed form [13]. The issues related to model-dependent studies of the dark energy EOS are a greater problem for the high precision datasets expected from next-generation cosmological experiments, including distance measurements from a Joint Dark Energy Mission (JDEM [36]).

Instead of using a parameterized form for  $w(z)$ , one can utilize a variant of principal component analysis [14] to establish the EOS without relying on a specific parameter description of the underlying redshift evolution. This was applied by Huterer & Cooray [15] to a set of early supernova data. More recently Riess et al. [7] used the same approach to analyze a new

set of  $z > 1$  SNe from the Hubble Space Telescope, while an analysis involving a larger combined dataset [16] has been presented in Sullivan et al. [17]. Here we use this model-independent approach to study the extent to which future data will constrain dark energy. We find that more than two independent parameters of the EOS can be determined with next-generation surveys. Our results argue against claims in the literature that next-generation surveys can only determine two parameters of the EOS as a function of redshift [18] and we motivate a model-free approach to study dark energy.

To encapsulate the range of possible future dark energy surveys, we consider six different data scenarios and generate mock data for each one assuming a flat  $\Lambda$ CDM cosmological model [4]. Our datasets are:

- Case A: A catalog of 200 SNe uniformly distributed in redshift out to  $z = 1.8$ ; in addition, two BAO distance estimates at  $z = 0.2$  and  $z = 0.35$ , with 6% and 4.7% uncertainties, respectively. This case approximates the current state of the data in SNe [7, 8, 16] and BAOs [3, 19].
- Case B: A catalog of 300 SNe uniformly distributed out to  $z = 0.1$ , as expected from ground-based low redshift samples, and an additional 2,000 SNe uniformly distributed in the range  $0.1 < z < 1.8$ , as expected from *JDEM* or similar future surveys [37]. In addition to the two BAO distances described in Case A, five additional BAO constraints at  $z = [0.6, 0.8, 1.0, 1.2, 3.0]$  with corresponding fiducial survey precisions of  $[4.3, 3.2, 2.3, 2.0, 1.2]\%$  ( $V_{1N1}$  from [20]).
- Case C: The same SN dataset as described in case B, the seven BAO estimates as described in case B, and, in addition, ten new BAO constraints expected from a proposed JDEM mission by NASA or ESA concentrating primarily on BAO measurements, such as *ADEPT* (Advanced Dark Energy Physics Telescope). These BAO estimates have precision (in  $D_V$  [3]) of

[0.36, 0.33, 0.34, 0.33, 0.31, 0.33, 0.32, 0.35, 0.37, 0.37]% from  $z = 1.05$  to  $1.95$  in steps of  $0.05$  [21].

- Case D: A dataset of 10,000 SNe uniformly distributed out to  $z = 2$ . In addition, seven BAO constraints as in case B, but assuming stronger accuracies (V5N5 of [20]) for the five higher-redshift BAO constraints: [1.9, 1.5, 1.0, 0.9, 0.6]% at  $z = [0.6, 0.8, 1.0, 1.2, 3.0]$ .
- Case E: The 10,000 SN dataset along with the seven BAO constraints as described in case D and the additional 10 BAO constraints expected from space-based missions as described in case C.
- Case F: The SN dataset as described in case A combined with the BAO estimates in case E.

For each of the cases listed above we create mock catalogs of SN and BAO observations. For each individual SN we simulate a random distance modulus  $m(z) - \mathcal{M}$  consistent with our fiducial cosmological model. In cases A to C, we bin the Hubble diagram at  $z > 0.1$  into 50 redshift bins, while the 10,000 SNe sample in cases A to F is binned into 500 bins. The error in distance modulus for each SN bin is given by  $\sigma_m = \sqrt{(\sigma_{\text{int}}/\sqrt{N_{\text{bin}}})^2 + \delta m^2}$ , where  $\sigma_{\text{int}} = 0.1$  mag is the intrinsic error for each SN [22],  $N_{\text{bin}}$  is the number of SNe in the redshift bin, and  $\delta m$  is the irreducible systematic error. We take the systematic error to have the form  $\delta m = 0.02(0.1/\Delta z)^{1/2}(1.7/z_{\text{max}})(1+z)/2.7$ , where  $z_{\text{max}}$  is the redshift of the furthest SNe, and  $\Delta z$  is the width of the relevant redshift bin. This is equivalent to the form in [23]. In addition, we include the effects of gravitational lensing magnification [24, 25, 26], although the noise from lensing is expected to be small for large datasets due to sample averaging [27, 28]. We make use of the probability distribution function for lensing magnification from Wang, Holz, & Munshi [29] at  $z \geq 0.6$ , while for SNe at  $z < 0.6$  we approximate the lensing by a Gaussian distribution for magnification with dispersion  $0.093z$  magnitudes, as given in Holz & Linder [28].

We analyze a set of 10 independent mock catalogs for the data cases B and C, to account for random variations in the estimates of the EOS. When model fitting each of the mock samples, we follow [7] and marginalize over a prior in  $\Omega_m h$  ( $0.213 \pm 0.023$  [30]), a prior in  $H_0$  ( $72 \pm 8$  km s $^{-1}$  Mpc $^{-1}$  [31]), and a prior in the distance to the last scattering surface at  $z = 1089$  ( $R = 1.71 \pm 0.03$  [32]). In order to account for uncertainty in the absolute magnitude, we also marginalize over the nuisance parameter,  $\mathcal{M}$ , with a uniform prior of  $-0.6$  to  $0.6$  [6]. To explore the importance of our fiducial assumption of a flat universe, for cases C and E we also explore a curvature prior, with a  $1\sigma$  uncertainty on  $\Omega_k$  of  $0.0032$  [33].

We refer the reader to Sullivan et al. [17] for details of our approach. We make use of a modified version

of the publicly available *wzbinned* code [38], which analyzes observational cosmological data via a Markov Chain Monte Carlo (MCMC) likelihood approach to estimate  $w(z)$  in redshift bins. In this parameterization, the EOS is taken to be constant in each redshift bin, but can vary from bin to bin. We take a total of six bins between  $z = 0$  and  $z = 3$  and fix the EOS at higher redshift to a constant value of  $-1$  out to the CMB at  $z = 1089$ . In addition, we also impose a prior on our furthest (6th) bin:  $-5 \leq w_6 \leq 0$ . This bin remains largely unconstrained by the data cases we have studied, and the prior facilitates convergence. In what follows we will generally omit this bin, as it is poorly constrained. The redshift intervals of the first five bins are listed in Table 1 and the intervals are chosen so that the error on  $w(z_i)$  is spread evenly across all bins.

The integration to higher redshifts causes correlations between lower- and higher-redshift  $w_i(z)$  bins, and this must be taken into account in the subsequent analysis. These correlations are encapsulated in the covariance matrix, which can be generated by taking the average of the Markov chain,  $C = \langle \mathbf{w}\mathbf{w}^T \rangle - \langle \mathbf{w} \rangle \langle \mathbf{w}^T \rangle$ , where  $\mathbf{w}$  captures estimates of  $w_i(z)$  as a vector. This covariance matrix is non-diagonal, with correlations between adjacent bins that slowly decrease with increasing bin separation.

Instead of restricting ourselves to correlated values of  $w_i(z)$ , we follow Huterer & Cooray [15] and decorrelate the EOS estimates. This is achieved by changing the basis through an orthogonal matrix rotation that diagonalizes the inverse covariance matrix. The Fisher matrix  $\mathbf{F} \equiv C^{-1}$  is then  $\mathbf{F} = \mathbf{O}^T \Lambda \mathbf{O}$  where the matrix  $\Lambda$  is the diagonalized inverse covariance of the transformed bins. The uncorrelated parameters are then defined by the rotation performed by the orthogonal matrix:  $\mathbf{q} = \mathbf{O}\mathbf{w}$ .

There is a freedom of choice in the orthogonal matrix used to perform this transformation. We follow the approach advocated in [15] and write the weight transformation matrix as  $\tilde{\mathbf{W}} = \mathbf{O}^T \Lambda^{\frac{1}{2}} \mathbf{O}$ , where the rows are summed such that the weights from each band add up to unity. This choice ensures we have mostly positive contributions across all bands, an intuitively pleasing result. We apply the transformation  $\tilde{\mathbf{W}}$  to each link in the Markov chain to generate a set of independent, uncorrelated measures of the probability distribution of the EOS in each bin as determined by the observables. We denote these uncorrelated bins as  $\tilde{\mathbf{w}} = \tilde{\mathbf{W}}\mathbf{w}$ . When discussing our results, we will generally refer to these uncorrelated estimates.

The results of our analysis are summarized in Table I. For each of the observational scenarios we give the  $1\sigma$  errors on the determination of  $w$  in 5 uncorrelated redshift ‘bins’. Since the redshift bins are decorrelated, they now leak into one another; the new window functions are shown in Fig. 1 where we illustrate the ex-

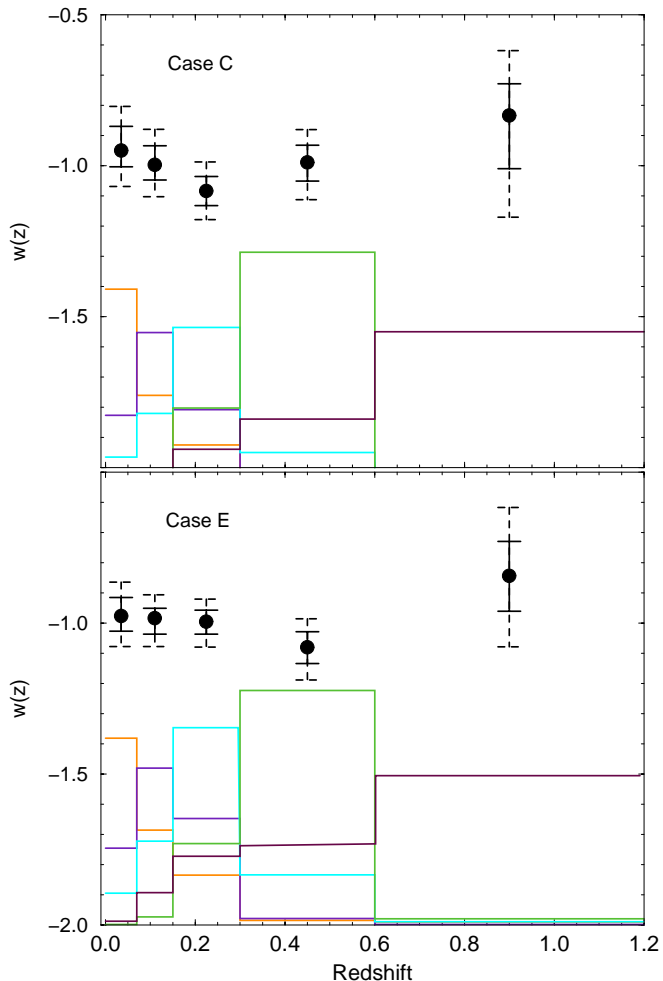


FIG. 1: Uncorrelated binned estimates of the EOS from a typical mock sample generated for Case C (top panel) and Case E (bottom panel). The error bars show  $1\sigma$  and  $2\sigma$  uncertainties with solid and dashed lines, respectively. At the bottom, in separate colors, we show the window function for each of the independent, decorrelated bins. The overlap in window functions represents the relative contribution from adjacent redshifts bins to each uncorrelated  $w(z_i)$  estimate.

pected errors in  $w(z_i)$  for two mock samples from Cases C and E. For Cases B and C we also list the relative dispersion of the binned  $w(z)$  errors determined by analyzing 10 independent datasets. For Case C we find that the first four bins have average errors of 0.067, 0.056, 0.048, and 0.059. Analyzing several independent mock catalogs, we found the standard deviation to be [3.3, 1.6, 2.5, 2.9]%, respectively for the first four bins, relative to the mean error. In the last column of Table I, we specify the number ( $N_P$ ) of *independent* EOS parameters that could be determined, according to our analysis, to an accuracy better than 10%. This is the same criteria used previously to argue that next-generation surveys can determine at most two parameters of the EOS [18].

Our results show that it is possible to determine *four*

Bin z range	$w_1(z)$	$w_2(z)$	$w_3(z)$	$w_4(z)$	$w_5(z)$	$N_P$
0-0.07	0.192	0.151	0.114	0.130	0.192	0
Case A	0.077	0.066	0.061	0.084	0.230	4
Case B	(1.9%)	(2.2%)	(1.8%)	(5.2%)	(12.8%)	
Case C	0.067	0.056	0.048	0.059	0.153	4
with $\Omega_K$	(3.3%)	(1.6%)	(2.5%)	(2.9%)	(8.1%)	
Case D	0.073	0.060	0.053	0.065	0.179	4
Case E	0.059	0.051	0.048	0.072	0.193	4
with $\Omega_K$	0.055	0.044	0.040	0.052	0.116	4
Case F	0.059	0.048	0.044	0.058	0.147	4
Case F	0.147	0.103	0.072	0.066	0.124	2

TABLE I: 68% error in the value of  $w$  in the uncorrelated redshift bins assuming a flat universe. The  $z$  range lists the redshift ranges for the original bins, but decorrelating the covariance matrix results in a leakage across bins. We show this leakage in the window functions in Figure 1 for two mock samples from cases C and E. The last column is the number of *independent* EOS parameters that could be determined to an accuracy better than 10%, consistent with a prior study [18]. For cases B and C, within brackets, we list the scatter relative to the mean error of  $w_i(z)$  using a moderate number of random datasets corresponding to the two cases. For cases C and E, we also show the errors for the case where we allow for variations in curvature with a prior on  $\Omega_K$  expected from Planck.

*independent* EOS parameters to an accuracy better than 10%, for the case of 2300 SNe coupled with high precision BAO measurements (e.g., Case C; Fig. 1). With cases D and E, two of these four parameters are determined with an accuracy at the level of 5%. Finally, we note that the results of case F show that even with only 200 SNe combined with future BAO measurements, one can constrain three independent EOS parameters to around 10%.

The results in Table 1 are for the case of a flat universe, except for an additional analysis of cases C and E with the inclusion of a Planck prior on the curvature [33]. With varying curvature, we find that the errors on  $w(z)$  broaden by less than 3% relative to the errors with the flat universe assumption. Thus the assumption of flatness, although it very slightly improves our fits, does not alter the general conclusion that one can constrain more than three parameters of the dark energy EOS.

Linder & Huterer [18] have argued that future data (SNe, CMB, and weak lensing measurements) will lead to a determination of no more than two independent parameters of the EOS to better than 10%. They consider a principal components analysis of the EOS binned at redshift intervals of 0.05, and argue that only the first two components are determined to better than 10%. While the third and higher principal components are determined individually with less accuracy, by combining multiple components additional indepen-

dent precise  $w(z_i)$  estimates can be achieved. Our approach utilizes much wider (and uneven) binning in redshift, thereby allowing for a more robust capture of dark energy properties, and thus naturally finding multiple independent parameters. In addition, while [18] limited themselves to a Fisher matrix approach, we explicitly generate mock data sets, accounting for intrinsic scatter and systematic biases such as lensing. Even with the inclusion of additional systematic errors, we find that future data constrain more than two independent parameters of the dark energy equation of state.

Two-parameter dark energy fitting has been incorporated into the figure-of-merit (FoM) quantity advocated by the Dark Energy Task Force [34], which is based on a two-parameter model for the equation of state ( $w(z) = w_0 + w_a(1 - a)$ ). This provides a convenient criterion for the evaluation of next-generation dark energy surveys. As an alternative, more general FoMs, such as the ones discussed in Albrecht & Bernstein [35] and Sullivan et al. [17], allow for more than two parameters. Since different FoMs highlight different aspects of the theory and the data, consideration of a range of FoMs is warranted.

In summary, we find that next-generation dark energy surveys will be able to constrain three or more independent parameters of the equation of state to an accuracy better than 10%. This is in contrast to recent claims in the literature, and conventional wisdom, that two parameters are sufficient in dark energy analyses. As we enter an era of precision measurements, it is important to avoid prejudicing our results with arbitrary functional forms for the dark energy. We have thus proposed a model-independent, multi-parameter analysis procedure for fitting the dark energy equation of state, and have shown that precision measurements of the dark energy can be expected with the next generation of surveys.

We thank an anonymous referee and Adam Riess for valuable comments. This work was supported by LANL IGPP Astro-1603-07, NSF CAREER AST-0645427 (AC) and a Richard P. Feynman Fellowship from LANL (DEH). AC and DEH thank Aspen Center for Physics for hospitality while this work was completed.

- 
- [1] A. G. Riess *et al.*, *Astrophys. J.* **607**, 665 (2004).  
 [2] J. L. Tonry *et al.*, *Astrophys. J.* **594**, 1 (2003).  
 [3] D. J. Eisenstein *et al.*, *Astrophys. J.* **633**, 560 (2005).  
 [4] D. N. Spergel *et al.*, *Astrophys. J. Suppl.* **170**, 377 (2007).

- [5] A. Riess *et al.*, *Astron. J.* **116**, 1009 (1998); S. Perlmutter *et al.*, *Astrophys. J.* **517**, 565 (1999).  
 [6] W. M. Wood-Vasey *et al.*, *Astrophys. J.* **666**, 694 (2007).  
 [7] A. G. Riess *et al.*, *Astrophys. J.* **659**, 98 (2007).  
 [8] P. Astier *et al.*, *Astron. Astrophys.* **447** 31 (2006).  
 [9] T. Padmanabhan, *Phys. Rept.* **380**, 235 (2003).  
 [10] A. R. Cooray and D. Huterer, *Astrophys. J.* **513**, L95 (1999) [arXiv:astro-ph/9901097].  
 [11] M. Chevallier and D. Polarski, *Int. J. Mod. Phys. D* **10**, 213 (2001).  
 [12] E.V. Linder *Phys. Rev. Lett.* **90**, 091301 (2003).  
 [13] B. F. Gerke and G. Efstathiou, *Mon. Not. Roy. Astron. Soc.* **335**, 33 (2002); C. Li, D. E. Holz and A. Cooray, *Phys. Rev. D* **75**, 103503 (2007).  
 [14] D. Huterer and G. Starkman, *Phys. Rev. Lett.* **90**, 031301 (2003).  
 [15] D. Huterer and A. Cooray, *Phys. Rev. D* **71**, 023506 (2005) [arXiv:astro-ph/0404062].  
 [16] T. M. Davis *et al.*, *Astrophys. J.* **666**, 716 (2007)  
 [17] S. Sullivan, A. Cooray, and D. E. Holz, *J. Cosmol. Astropart. Phys.* 09 (2007) 004  
 [18] E. V. Linder and D. Huterer, *Phys. Rev. D* **72**, 043509 (2005).  
 [19] W. J. Percival *et al.*, *Mon. Not. R. Astron. Soc.* **381**, 1053 (2007)  
 [20] H-J. Seo and D. J. Eisenstein, *Astrophys. J.* **598**, 720 (2003).  
 [21] A. Riess (private communication).  
 [22] A. G. Kim, E. V. Linder, R. Miquel and N. Mostek, *Mon. Not. Roy. Astron. Soc.* **347**, 909 (2004).  
 [23] E. V. Linder and D. Huterer, *Phys. Rev. D* **67**, 081303 (2003).  
 [24] J. A. Frieman, arXiv:astro-ph/9608068.  
 [25] D. E. Holz and R. M. Wald, *Phys. Rev. D* **58**, 063501 (1998).  
 [26] Y. Wang, *Astrophys. J.* **536**, 531 (2000)  
 [27] D. Sarkar, A. Amblard, D. E. Holz, and A. Cooray, *Astrophys. J.* **678**, 1 (2008) [arXiv:0710.4143].  
 [28] D. E. Holz and E. V. Linder, *Astrophys. J.* **631**, 678 (2005).  
 [29] Y. Wang, D. E. Holz, and D. Munshi, *Astrophys. J.* **572**, L15 (2002).  
 [30] M. Tegmark *et al.*, *Astrophys. J.* **606**, 702 (2004).  
 [31] W. L. Freedman *et al.*, *Astrophys. J.* **553**, 47 (2001).  
 [32] Y. Wang and P. Mukherjee, *Phys. Rev. D* **76**, 103533 (2007).  
 [33] K. M. Smith, W. Hu, and M. Kaplinghat, *Phys. Rev. D* **74**, 123002 (2006).  
 [34] A. Albrecht *et al.*, arXiv:astro-ph/0609591 (2006).  
 [35] A. Albrecht and G. Bernstein, *Phys. Rev. D* **75**, 103003 (2007).  
 [36] <http://universe.nasa.gov/program/probes/jdem.html>  
 [37] Our results are insensitive to the precise shape of the redshift distributions. Furthermore, a mission like *SNAP* (SuperNova Acceleration Probe) would find greater than 2,000 SNe, and a subset of the SNe with a uniform redshift distribution is expected for analysis.  
 [38] <http://www.cooray.org/sn.html>